



Estimation of background radiation in the indoor air in geo-sensitive zones of the Garhwal Himalaya, India

Ganesh Prasad¹ · Krishna Pal Singh² · Sanjeev Kimothi³ · Subhash Chandra² · R. C. Ramola⁴

Received: 1 September 2023 / Accepted: 19 December 2023 / Published online: 13 January 2024
© Akadémiai Kiadó, Budapest, Hungary 2024

Abstract

The study assesses environmental background radiation from radon, thoron, and thoron decay products across distinct geological settings in the Garhwal Himalaya region by using RADUET, CR-39 plastic track detectors, and deposition-based thoron (^{220}Rn) progeny detectors. The measurements were conducted indoors throughout the winter, summer, and rainfall seasons during the year 2013. The annual inhalation doses from ^{220}Rn progenies ranged between 0.83 and 2.99 mSv y^{-1} , averaging 1.94 mSv y^{-1} . The annual effective dose (AED), reflecting biological radiation impact, varied from 0.58 to 2.78 mSv y^{-1} , with an average of 1.75 mSv y^{-1} .

Keywords Radiation dosage · Toxicity · Effective dose · RADUET · CR-39

Introduction

In the context of the Himalayan tectonic settings, the undulating geological conditions play a pivotal role in influencing ambient background radiation. This radiation can encompass varying concentrations of radon, ranging from modest to severe levels. This is particularly concerning due to the potential release of significant decay products, which can pose harm to human health upon inhalation.

Radon (^{222}Rn) and thoron (^{220}Rn) are generated through the alpha decay of radium (^{226}Ra) in the uranium (^{238}U) decay series and radium (^{224}Ra) in the thorium (^{232}Th) decay series, respectively [1]. The distinct half-lives of ^{222}Rn (3.8 days) and ^{220}Rn (55.6 s) contribute to the differential distribution of residential sources. Specifically, ^{222}Rn primarily originates from the foundations and walls of rooms, while ^{220}Rn predominantly emerges from walls [2]. As both

radon types are emitted from the ground and walls, their decay products are released into the atmosphere. Upon inhalation, the decay products of ^{222}Rn and ^{220}Rn are deposited within the bronchial tree's airways, thus exposing the lungs [2, 3]. The entry of ^{222}Rn into indoor air occurs through minute cracks, fissures, and poorly sealed wall joints, thereby becoming accessible for inhalation and ingestion by individuals [4–7]. The difference in temperature between outdoor and indoor spaces generates a pressure gradient, facilitating the entry of ^{222}Rn into indoor air [6, 8]. Once inhaled, the densely ionizing alpha particles of ^{222}Rn interact with lung tissues, causing DNA damage that is associated with the development of lung cancer [1, 9, 10]

Remarkably, radon (^{222}Rn) stands as the primary contributor to public radiation exposure, accounting for more than half of the total radiation humans are exposed [2]. Elevated quantities of ^{222}Rn and its progenies within indoor spaces can pose substantial health risks. The alpha particles emitted by inhaled ^{222}Rn , particularly two of its progenies, polonium (^{214}Po and ^{218}Po), hold significant destructive potential for lung tissue and have been linked to the occurrence of lung cancer in humans [11]. The WHO [12] scaled ^{222}Rn as the second leading reason of lung cancer, among smokers, and as the leading cause among all non-smokers. Both ^{222}Rn and ^{220}Rn , along with their decay products, are widely acknowledged contributors to human natural background radiation exposure, accounting for more than 50% of the total. Additionally, the inhalation doses of ^{222}Rn and ^{220}Rn within

✉ Subhash Chandra
subhash.physics@gmail.com

¹ Department of Physics, B.L.J. Govt. P.G College, Purola, Uttarkashi 249185, India

² Department of Physics, P.N.G. Govt. P.G. College, Ramnagar, Nainital 244715, India

³ Department of Physics, Graphic Era Deemed to Be University, Dehradun 248002, India

⁴ Department of Physics, H.N.B. Garhwal University, Badshahi Thaul Campus, Tehri Garhwal 249199, India

indoor air are predominantly influenced by the concentrations of their decay products [3, 13, 14]. Indoor background radiation exposure and concentrations are impacted by factors such as ^{222}Rn exhalation rates, ventilation conditions, and building materials [15–19]. The results of the present study can aid in understanding the health concerns connected to radon and thorium exposure in related geological settings. The concentration data and related dose estimations can help in identifying potential dangers to health and formulating effective mitigation plans.

In past studies [10, 20–23], the contribution of ^{220}Rn inhalation and its decay products was often overlooked due to its short half-life. Notably, an investigation of gamma dose rates across forty-six locations in the Uttarakhand Himalayas, India, under various geological stresses, revealed moderate variations in dose rates [24]. Nevertheless, the higher dosage conversion ratio associated with ^{220}Rn decay products underscores its significance, particularly in scenarios characterized by elevated ^{220}Rn levels, such as homes constructed using materials rich in thorium. This current study aims to assess the environmental background radiation exposure resulting from the decay products of both ^{222}Rn and ^{220}Rn , within different dwelling materials in the geological settings of the Garhwal Himalayas.

Methodology

The experimental site is in the Central Himalayan region situated along the Himalayan Frontal Thrust (HFT) and the Main Boundary Thrust (MBT) regions, the most tectonically active regions. The geophysical and tectonic consequences are linked with the emission of soil gas. This experimental site is focused on frequent monitoring and in-depth investigation in accordance with the health concerns of residents.

In the present study in the tectonically active zone in the Garhwal Himalaya, different types of houses made up of different building materials were used. Therefore, the current study aimed to estimate the radiation doses received by the inhabitants due to ^{222}Rn , ^{220}Rn , and their progenies. The RADUET CR-39 films are used to record the presence of alpha particles in different dwellings of the experimental site. The detectors were placed in the bedrooms and the living rooms of the study regions at the 2 m height from the surface [25]. After the exposure of 3-months, these CR-39 films underwent a chemical etching process in a 6.25 normality NaOH solution at a temperature of 90 °C for a duration of 6 h. Following the etching process, the CR-39 films were subjected to analysis within an automated track-counting system. This analysis aimed to determine the density of alpha particle tracks. Subsequently, the ^{222}Rn concentrations were derived using different factors such as the density of background tracks, the duration of exposure, and

specific calibration factors. These calibration factors were established through exposure to both ^{222}Rn and ^{220}Rn utilizing specialized chambers located at the National Institute of Radiological Sciences, Japan. To ensure the quality and reliability of the detectors, inter-comparison was conducted. The minimum detection limit (MDL) used in the present study were 3 and 14 Bq m⁻³ for radon and thoron (if concentrations were supposed to be 40 and 100 Bq m⁻³) respectively and the MDL values depend on the obtained concentrations [26, 27].

The following formulae were used to calculate the indoor ^{222}Rn and ^{220}Rn concentrations [28, 29]:

$$C_T = (T_{Rn+Tn} - T_{Rn}) / (d \times k_{Tn}) \quad (1)$$

$$C_R = (T_{Rn}) / (d \times k_{Rn}) \quad (2)$$

where k_{Rn} and k_{Tn} stand for calibration factor for the ^{222}Rn (0.0172 ± 0.002 tracks.cm⁻²/Bq.m⁻³.d) and ^{220}Rn (0.010 ± 0.001 tracks.cm⁻²/Bq.m⁻³.d) respectively. C_T and C_R stand for the ^{220}Rn and ^{222}Rn concentrations (in Bq m⁻³), and T_{Rn} , T_{Rn+Tn} stand for the densities of the tracks in the “ ^{222}Rn ” and “ $^{222}\text{Rn} + ^{220}\text{Rn}$ ” chambers, respectively.

The indoor progeny concentration of the radon and thoron progeny can be calculated by the below equation [30, 31]:

$$\text{EETC} = T_{\text{DTPS}} / d \times S_{Tn} \quad (3)$$

$$\text{EERC} = (T_{\text{DRPS}} / d \times S_{Rn}) - \text{EETC} \quad (4)$$

where EERC and EETC stand for the equilibrium equivalent due to the concentration of the radon and thoron (Bq m⁻³). T_{DTPS} and T_{DRPS} stand for the densities of the tracks, S_{Tn} and S_{Rn} stand for sensitivity factors for DTSPS (0.09 trackscm⁻².d⁻¹/EERC (Bq m⁻³)) for DRPS (0.94 trackscm⁻².d⁻¹/EETC (Bq m⁻³)) respectively. The average value of the thoron progeny concentration for the same month was also derived from their exposure time and material categories of dwellings. The ^{220}Rn progeny (Bq m⁻³) concentration under different environmental settings was explored in the present study.

Equilibrium factors for thoron (^{220}Rn)

The radon (^{222}Rn) and thoron (^{220}Rn) equilibrium factors can be calculated by the below equation [32–35]:

$$F_{Rn} = \text{EERC} / C_R \quad (5)$$

$$F_{Tn} = \text{EETC} / C_T \quad (6)$$

where F_{Tn} and F_{Rn} stand for the equilibrium factors of thoron and radon. EERC, EETC, C_R , and C_T are in Bq m⁻³

as discussed above in Eqs. 3, 4, 1, and 2 respectively. In the present study, only the thoron equilibrium factor (F_{Tn}) was calculated due to not getting radon progenies concentrations.

Annual inhalation dose (D) and annual effective dose (AED) calculation

The annual inhalation dose (D) and annual effective dose (AED) of radon, thoron, and their progeny were estimated by the following equations [10, 21, 36, 37]:

$$D = [(0.17 + 9 \times F_{Rn})C_R + (0.11 + 40 \times F_{Tn})C_T] \times 0.8 \times 8760 \times 10^{-6} \quad (7)$$

$$(AED)_{Rn} = [(0.17 + 9 \times F_{Rn})C_R] \times 0.8 \times 8760 \times 10^{-6} \quad (8)$$

$$(AED)_{Tn} = [(0.11 + 40 \times F_{Tn})C_T] \times 0.8 \times 8760 \times 10^{-6} \quad (9)$$

where C_R and C_T are the annual indoor radon and thoron concentrations, respectively with an annual indoor occupancy factor of 0.8. $(AED)_{Rn}$ and $(AED)_{Tn}$ are the annual effective dose due to the concentrations of radon and thoron ($mSv\ y^{-1}$) respectively. F_{Rn} and F_{Tn} are the equilibrium factors explained in Eqs. 5 and 6 respectively [20, 38, 39].

Results and discussion

The radon and thoron concentration in the present study was carried out in the different houses of the different building materials. The first three of the samples (serial number 1–3) was measured in the houses made up of wood and stone, four of the samples from the houses made up of cement only (serial number 4, 5, 7, 11), three of the samples from the houses made up of wood and mud (serial number 8–10), and one sample from the house made up of wood and cement (serial number 6). Radon concentrations in all three season was found to be higher than other samples in the houses that are made up of cement only and mixed up with cement. The thoron concentrations were found to be higher than other samples in the houses made up of mixed wood. (wood+ stone in January to March and July to September, and wood + mud in April to June). The obtained concentrations are comparable to the other tectonically active zones [40–44]. Table 1 demonstrated the average value of ^{222}Rn and ^{220}Rn concentration ($Bq\ m^{-3}$) in different seasons during the sampling period with different exposure times. Annual average ^{222}Rn and ^{220}Rn concentrations have been estimated in different indoor environments and the statistical data of the study is presented here.

The season-wise values of the equilibrium factors for thoron with its annual average values are presented in Table 2.

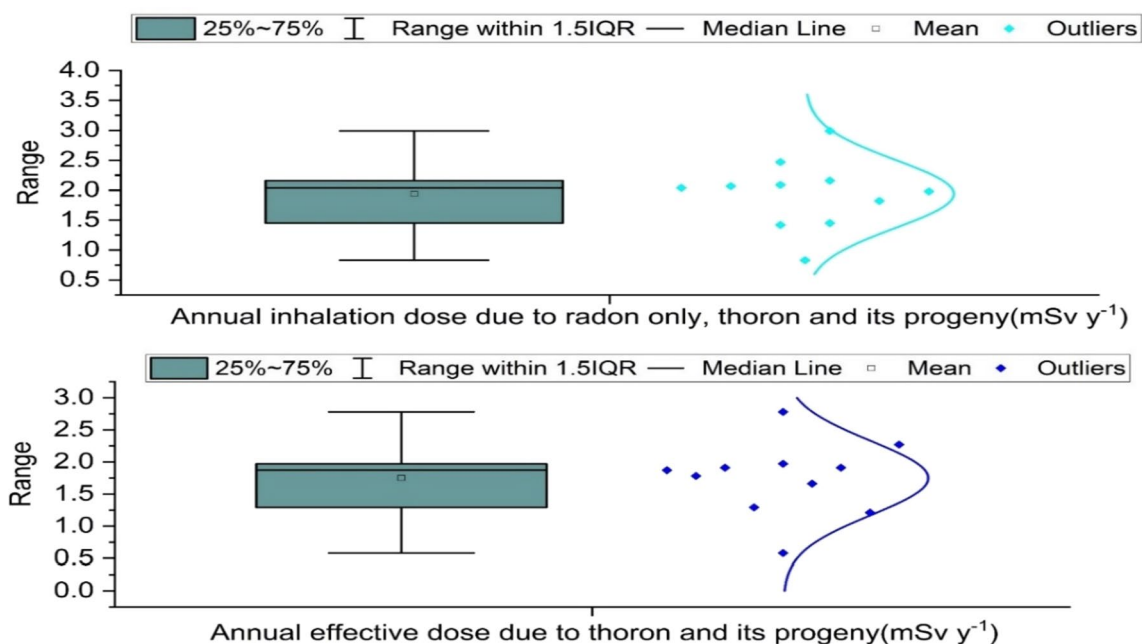
Table 1 The average value of ^{222}Rn and ^{220}Rn concentration ($Bq\ m^{-3}$) in different months of the year with their exposure time

Serial Number	January to March (Exposure time 95 Days)		April to June (Exposure time 101 Days)		July to October (Exposure time 92 Days)		Annual Average ^{222}Rn Con. ($Bq\ m^{-3}$)	Annual Average ^{220}Rn Con. ($Bq\ m^{-3}$)
	^{222}Rn Con. ($Bq\ m^{-3}$)	^{220}Rn Con. ($Bq\ m^{-3}$)	^{222}Rn Con. ($Bq\ m^{-3}$)	^{220}Rn Con. ($Bq\ m^{-3}$)	^{222}Rn Con. ($Bq\ m^{-3}$)	^{220}Rn Con. ($Bq\ m^{-3}$)		
1	124 ± 7	680 ± 32	N/A	N/A	188 ± 9	594 ± 43	156	637
2	128 ± 8	508 ± 31	168 ± 9	434 ± 36	N/A	N/A	148	471
3	116 ± 6	360 ± 24	133 ± 7	405 ± 28	169 ± 9	410 ± 34	139	392
4	122 ± 6	373 ± 26	148 ± 7	418 ± 31	149 ± 12	508 ± 36	140	433
5	120 ± 7	289 ± 29	142 ± 12	380 ± 35	157 ± 8	458 ± 34	140	376
6	144 ± 7	302 ± 26	170 ± 9	295 ± 32	204 ± 11	354 ± 40	173	317
7	170 ± 8	346 ± 31	161 ± 8	218 ± 28	203 ± 10	214 ± 35	178	259
8	134 ± 7	289 ± 25	168 ± 8	311 ± 30	182 ± 10	492 ± 38	161	364
9	137 ± 8	293 ± 32	128 ± 10	303 ± 28	185 ± 10	307 ± 33	150	301
10	190 ± 10	269 ± 33	147 ± 9	530 ± 34	N/A	N/A	169	400
11	260 ± 13	– 514 ± 35 (BDL)	160 ± 17	496 ± 43	219 ± 11	450 ± 51	213	144
Min	116	BDL	N/A	N/A	N/A	N/A	139	144
Max	260	680	170	530	219	594	213	637
AM	149.55	337.18	152.50	344.55	165.60	344.27	160.56	372.11
SD	43.08	165.76	48.16	146.86	62.05	198.73	22.09	125.58

BDL = Below Detection level, NA = Data Not Available, Min = Minimum, Max = Maximum, AM = Arithmetic Mean, SD = Standard Deviation

Table 3 Total annual inhalation dose due to radon only, ^{220}Rn and its progeny, and annual effective dose due to ^{220}Rn and its progeny (mSv y^{-1})

Serial Number	Annual inhalation dose due to radon only, thoron and its progeny (mSv y^{-1})	Annual effective dose due to thoron and its progeny (mSv y^{-1})
1	2.16	1.97
2	2.09	1.91
3	1.82	1.66
4	2.07	1.91
5	1.45	1.29
6	2.99	2.78
7	1.42	1.21
8	1.98	1.78
9	2.04	1.87
10	2.47	2.27
11	0.83	0.58

**Fig. 2** Box and Whisker plot for annual inhalation dose due to radon only, thoron and its decay product (upper part), and annual effective dose (lower part) due to thoron and its decay product

thoron and its decay product. It can be seen from the Figure that a similar trend was followed by both the parameters in which the maximum value was obtained at approximately 3 mSv y^{-1} and the minimum value was obtained between 0.5 to 1 mSv y^{-1} .

The correlation coefficient for annual inhalation dose caused by radon only, thoron and its decay product (right side), and annual effective dose caused by thoron and its decay product (left side) within the annual average equilibrium factor (F_{Tn}) are shown in Fig. 4. The Pearson's r value between annual effective dose caused by radon only, thoron and its decay product and annual average equilibrium

factor (F_{Tn}) was found 0.65 (p values = 0.027) whereas between annual effective dose due to thoron and its decay product and annual average equilibrium factor (F_{Tn}) was found 0.63 (p values = 0.034). Both of the parameters showed a strong correlation with the annual average equilibrium factor. The p values showed that the correlation between the above parameters is significant.

The correlation coefficient of the annual inhalation dose caused by radon only, thoron, and its decay product (right side), as well as the annual effective dose caused by thoron and its decay product, has been analyzed as shown in Fig. 5. It can be seen from the Figure

Fig. 3 Line and symbol plot for annual inhalation dose caused by radon only, thoron and its decay product (upper part), and annual effective dose (lower part) caused by thoron and its decay product

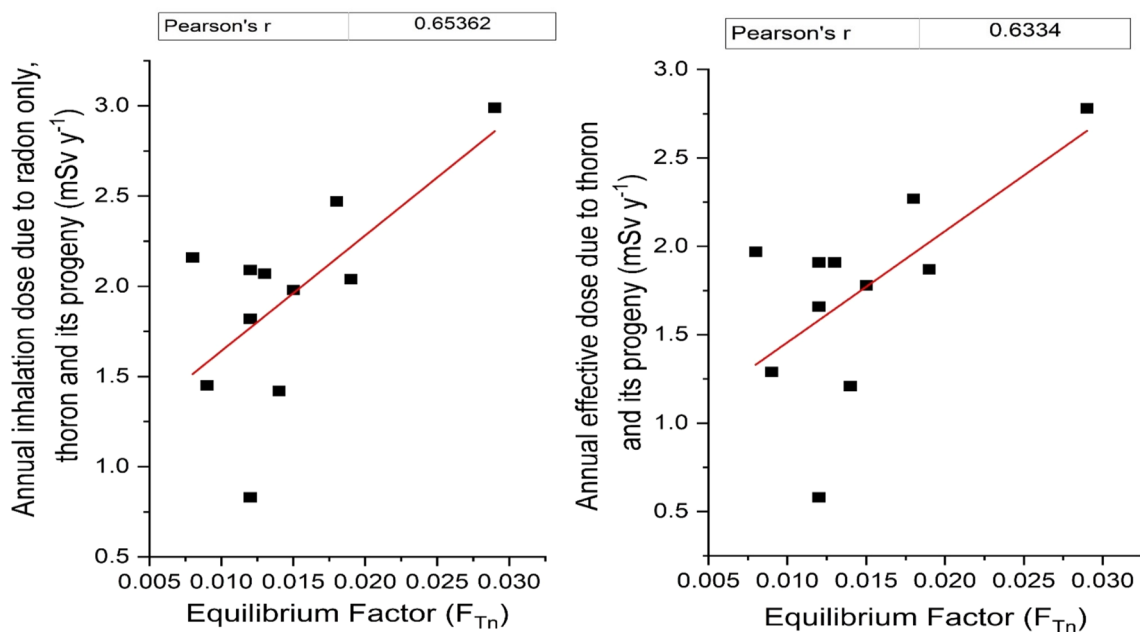
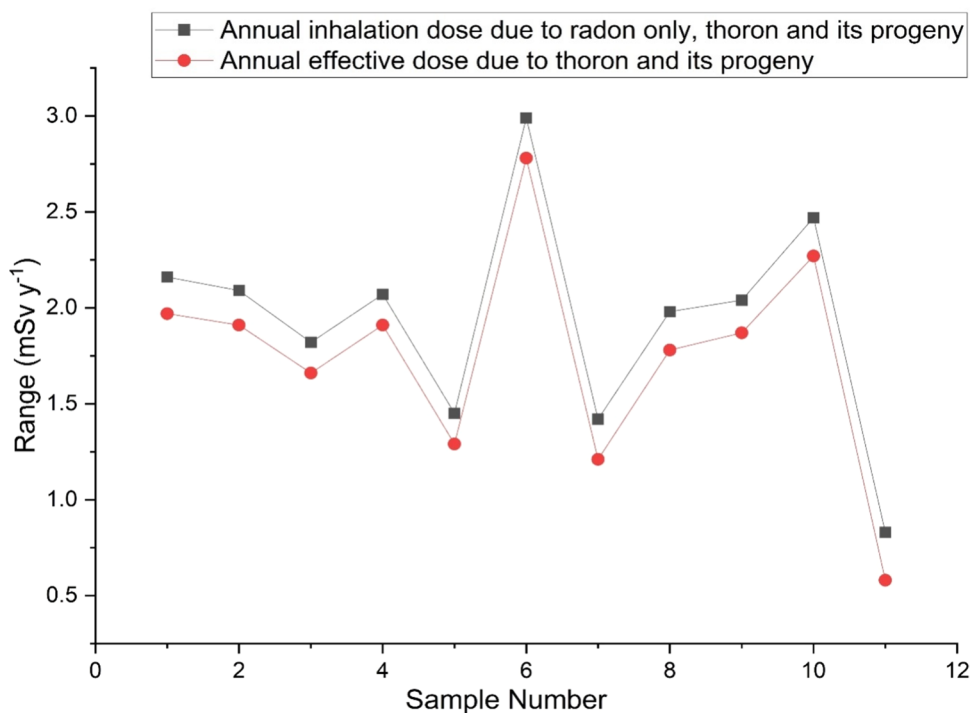


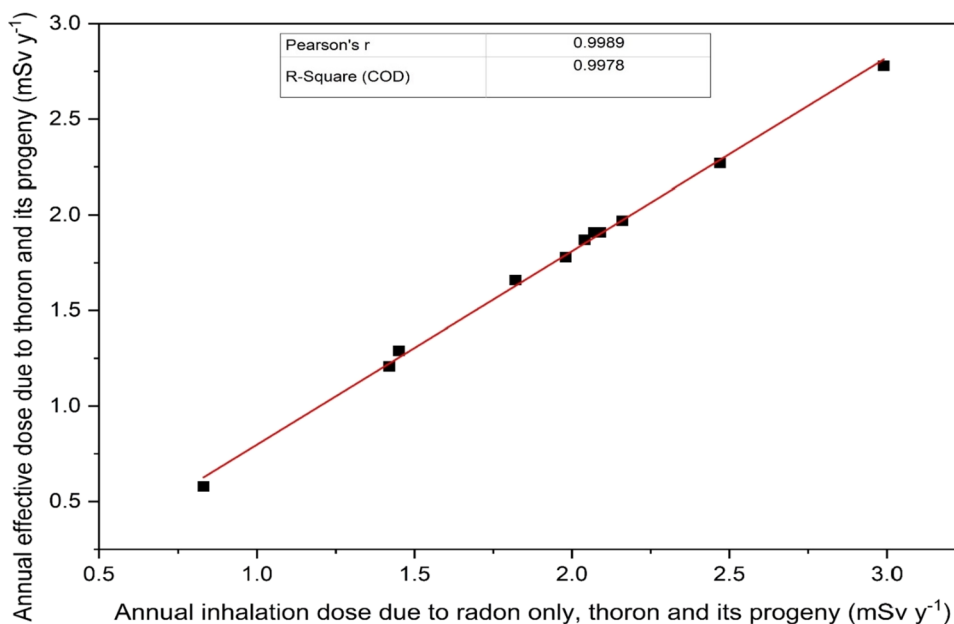
Fig. 4 Correlation coefficient for annual inhalation dose (right side) and annual effective dose (left side) within annual average equilibrium factor (F_{Tn})

that a strong positive correlation coefficient (Pearson's r value = 0.99) was obtained between them which means that there is a linear relationship between these two parameters.

Conclusions

The current study indicates that both (radon and thoron) indoor concentrations and equilibrium equivalent radon and thoron concentrations change considerably with season. The

Fig. 5 Correlation coefficient relationships among annual inhalation dose due to radon only, thoron and its progeny, and annual effective dose due to



indoor radon and thoron concentrations observed are higher than the World Health Organization (WHO) suggested guideline level of 100 Bq m^{-3} as a consequence of the inadequate ventilation and low humidity, the projected seasonal value of the equilibrium factor for thoron and its offspring (F_{Th}) is highest in the winter and lowest in the summer. The average yearly radon, thoron, and their offspring inhalation exposure is much lower than the UNSCEAR-suggested reference level. The calculated annual radon effective dosage is below the WHO and ICRP reference limits in the specific geographical area of the Garhwal Himalaya region, these dose assessments offer useful baseline information on radon and thoron exposure levels.

Declarations

Conflict of interest The authors declare that they have no conflict of interest in the present manuscript.

References

- Krishna Pal Singh, Subhash Chandra et al (2023) Measurement of radon concentration in soil gas and radon exhalation rate from soil samples along and across the Main Central Thrust of Garhwal Himalaya, India. *Environ Geochem Health* 45:8771–8786. <https://doi.org/10.1007/s10653-023-01758-7>
- UNSCEAR (2000) Sources and effects of ionizing radiation, United Nations scientific committee on the effects of atomic radiation UNSCEAR 2000 report to the general assembly, with scientific annexes volume i: sources united nations. New York
- United Nations. Scientific Committee on the Effects of Atomic Radiation. (2010) Sources and effects of ionizing radiation : United Nations Scientific Committee on the Effects of Atomic Radiation : UNSCEAR 2008 report to the General Assembly, with scientific annexes. United Nations
- Jantsikene A, Kiisk M, Suursoo S et al (2014) Groundwater treatment as a source of indoor radon. *Appl Radiat Isot* 93:70–75. <https://doi.org/10.1016/J.APRADISO.2014.01.006>
- Ramola RC, Gusain GS, Rautela BS et al (2016) Levels of thoron and progeny in high background radiation area of southeastern coast of Odisha, India. *Radiat Prot Dosim* 152:62–65. <https://doi.org/10.1093/rpd/ncs188>
- Pant P, Kandari T, Prasad M, Ramola RC (2016) A comparative study of diurnal variation of radon and thoron concentrations in indoor environment. *Radiat Prot Dosimetry* 171:212–216. <https://doi.org/10.1093/rpd/ncw061>
- Abbasi A, Algethami M, Bawazeer O, Zakaly HMH (2021) Wind-catcher ventilation computation and indoor ^{222}Rn concentration in traditional adobe houses. *Radiat Prot Dosimetry* 197:175–182. <https://doi.org/10.1093/RPD/NCAB178>
- Maghraby AM, Alzimami K, Abo-Elmagd M (2014) Estimation of the residential radon levels and the population annual effective dose in dwellings of Al-kharj, Saudi Arabia. *J Radiat Res Appl Sci* 7:577–582. <https://doi.org/10.1016/J.JRRAS.2014.09.013>
- Singh KP, Chandra S, Prasad M et al (2023) Estimation of radiation dose due to ingestion of radon in water samples of Garhwal Himalaya. *J Radioanal Nucl Chem, India*. <https://doi.org/10.1007/s10967-023-09002-3>
- Semwal P, Agarwal TK, Joshi M et al (2023) Effective dose estimation of radon, thoron and their progeny concentrations in the environs of Himalayan belt, India. *Int J Environ Sci Technol* 20:4127–4138. <https://doi.org/10.1007/s13762-022-04118-7>
- Ferlay J, Autier P, Boniol M et al (2007) Estimates of the cancer incidence and mortality in Europe in 2006. *Ann Oncol* 18:581–592. <https://doi.org/10.1093/annonc/mdl498>
- World Health Organization (2017) WHO guidelines for the drinking water. *World health Statistics* 1–116
- Bourai AA, Aswal S, Dangwal A et al (2013) Measurements of radon flux and soil-gas radon concentration along the main central thrust, Garhwal Himalaya, using SRM and RAD7 detectors. *Acta Geophys* 61:950–957. <https://doi.org/10.2478/S11600-013-0132-2/METRICS>
- Shahrokhii A, Adelikhah M, Imani M, Kovács T (2021) A brief radiological survey and associated occupational exposure to

- radiation in an open pit slate mine in Kashan Iran. *J Radioanal Nucl Chem* 329:141. <https://doi.org/10.1007/s10967-021-07778-w>
15. Etiopie G, Martinelli G (2002) Migration of carrier and trace gases in the geosphere: an overview. *Phys Earth Planet Inter* 129:185–204. [https://doi.org/10.1016/S0031-9201\(01\)00292-8](https://doi.org/10.1016/S0031-9201(01)00292-8)
 16. Kemski J, Klingel R, Siehl A, Valdivia-Manchego M (2009) From radon hazard to risk prediction-based on geological maps, soil gas and indoor measurements in Germany. *Environ Geol* 56:1269–1279. <https://doi.org/10.1007/S00254-008-1226-Z/METRICS>
 17. Rautela BS, Yadav M, Bourai AA et al (2012) Study of natural radionuclide and absorbed gamma dose in ukhimath area of garhwal Himalaya, India. *Radiat Prot Dosimetry* 152:58–61. <https://doi.org/10.1093/rpd/ncs187>
 18. Yadav M, Prasad M, Joshi V et al (2016) A comparative study of radium content and radon mass exhalation rate from soil samples using active and passive techniques a comparative study of radium content and radon exhalation rate from soil samples using active and passive techniques. *Radiat Prot Dosimetry* 171:254–256. <https://doi.org/10.1090/rpd/ncw069>
 19. Kandari T, Prasad M, Pant P et al (2018) Study of radon flux and natural radionuclides (^{226}Ra , ^{232}Th and ^{40}K) in the main boundary thrust region of Garhwal Himalaya. *Acta Geophys* 66:1243–1248. <https://doi.org/10.1007/s11600-018-0158-6>
 20. Ramola R (2016) Dose estimation derived from the exposure to radon, thoron and their progeny in the indoor environment. *Nature Sci Rep* 6:31061
 21. Prasad M, Bossew P, Anil Kumar G et al (2018) Dose assessment from the exposure to attached and unattached progeny of radon and thoron in indoor environment. *Acta Geophysica* 66:1187. <https://doi.org/10.1007/s11600-018-0111-8>
 22. Panwar P, Joshi A, Prasad M, Ramola RC (2022) Radiological dose estimation due to exposure to attached and unattached fractions of radon and thoron progeny concentrations. *J Radioanal Nucl Chem* 331:1024. <https://doi.org/10.1007/s10967-021-08103-1>
 23. Keramati H, Ghorbani R, Fakhri Y et al (2018) Radon 222 in drinking water resources of Iran: A systematic review, meta-analysis and probabilistic risk assessment (Monte Carlo simulation). *Food Chem Toxicol* 115:460–469. <https://doi.org/10.1016/J.FCT.2018.03.042>
 24. Prasad G, Kimothi S, Chandra S et al (2022) Monitoring of terrestrial gamma radiation exposure in different geological Stress conditions of Uttarakhand Himalayan region. *India J Phys Conf Ser* 2267:012102. <https://doi.org/10.1088/1742-6596/2267/1/012102>
 25. Prasad G, Kimothi S, Chandra S, et al Doses from inhalation of radon and thoron for residents in tectonically active region in central Indian Himalaya. SpringerG Prasad, S Kimothi, S Chandra, Y Omori, SK Sahoo, T Ishikawa, S Tokonami, RC Ramola *Journal of Radioanalytical and Nuclear Chemistry*, 2023•Springer
 26. Ramola RC, Prasad G, Gusain GS et al (2010) Preliminary indoor thoron measurements in high radiation background area of south-eastern coastal Orissa, India. *Radiat Prot Dosimetry* 141:379–382. <https://doi.org/10.1093/RPD/NCQ238>
 27. Tokonami S, Takahashi H, Kobayashi Y et al (2005) Up-to-date radon-thoron discriminative detector for a large scale survey. *Rev Sci Instrum* 76:1–5. <https://doi.org/10.1063/1.2132270/352833>
 28. Ramola RC, Prasad M, Rawat M et al (2015) Comparative study of various techniques for environmental radon, thoron and progeny measurements. *Radiat Prot Dosimetry* 167:22–28. <https://doi.org/10.1093/rpd/ncv215>
 29. Joshi V, Dutt S, Yadav M et al (2016) Measurement of radon, thoron and their progeny concentrations in the dwellings of Pauri Garhwal, Uttarakhand, India. *Radiat Prot Dosimetry* 171:234–237. <https://doi.org/10.1093/rpd/ncw065>
 30. Kumar A, Sharma S, Mehra R et al (2017) Assessment of indoor radon, thoron concentrations, and their relationship with seasonal variation and geology of Udhampur district, Jammu & Kashmir, India. *Int J Occup Environ Health* 23:202–214. <https://doi.org/10.1080/10773525.2018.1450326>
 31. Kandari T, Aswal S, Prasad M et al (2016) Study of radiation exposure due to radon, thoron and their progeny in the indoor environment of Rajpur region of Uttarakhand Himalaya. *Radiat Prot Dosim*. <https://doi.org/10.1093/rpd/ncw059>
 32. Prasad M, Rawat M, Dangwal A et al (2016) Study of radiation exposure due to radon, thoron and progeny in the indoor environment of Yamuna and Tons Valleys of Garhwal Himalaya. *Radiat Prot Dosim* 171:187–191. <https://doi.org/10.1093/rpd/ncw055>
 33. Mishra R, Sapra BK, Mayya YS (2014) Multi parametric approach towards the assessment of radon and thoron progeny exposure. *Rev Sci Instrum* 85:022105. <https://doi.org/10.1063/1.4865165>
 34. Prasad M, Rawat M, Dangwal A et al (2016) Variability of radon and thoron equilibrium factors in indoor environment of Garhwal Himalaya. *J Environ Radioact* 151:28. <https://doi.org/10.1016/j.jenvrad.2015.10.017>
 35. Nader AF (2019) The determination of equilibrium factor of radon and thoron using LR-115 type II detector in a selected area from Basra Governorate. *Iraq J Phys Confer Ser* 1258:12032
 36. Ramola RC, Prasad M, Kandari T et al (2016) Dose estimation derived from the exposure to radon, thoron and their progeny in the indoor environment. *Sci Rep* 6:31061. <https://doi.org/10.1038/srep31061>
 37. Kumar A, Singh P, Agarwal T et al (2020) Statistical inferences from measured data on concentrations of naturally occurring radon, thoron, and decay products in Kumaun Himalayan belt. *Environ Sci Pollut Res* 27:40229. <https://doi.org/10.1007/s11356-020-09920-9>
 38. Mehra R, Jakhu R, Bangotra P et al (2016) Assessment of inhalation dose from indoor ^{222}Rn and ^{220}Rn using RAD7 and Pinhole cup dosimeters. *Radiat Prot Dosim* 171:287–289. <https://doi.org/10.1093/rpd/ncw060>
 39. Mehra R, Bangotra P, Kaur K et al (2015) Estimation of attached and unattached progeny of ^{222}Rn and ^{220}Rn concentration using deposition based progeny sensors. *Radiat Prot Dosim* 167:92–96. <https://doi.org/10.1093/rpd/ncv223>
 40. Choubey VM, Ramola RC (1997) Correlation between geology and radon levels in groundwater, soil and indoor air in Bhilangana Valley, Garhwal Himalaya, India. *Environ Geol* 32:258–262. <https://doi.org/10.1007/s002540050215>
 41. Kumar G, Bhadwal R, Kumar M et al (2022) Radioactivity monitoring in the vicinity of Jawalamukhi thrust NW Himalaya, India for tectonic study. *Nat Hazards* 111:2219–2240. <https://doi.org/10.1007/S11069-021-05134-5>
 42. Al-Hilal M, Abdul-Wahed MK (2016) Tectonic and geologic influences on soil gas radon emission along the western extension of Damascus fault, Syria. *Environ Earth Sci* 75:1–11. <https://doi.org/10.1007/S12665-016-6292-Z/METRICS>
 43. Przylibski TA, Zebrowski A, Karpińska M et al (2011) Mean annual ^{222}Rn concentration in homes located in different geological regions of Poland – first approach to whole country area. *J Environ Radioact* 102:735–741. <https://doi.org/10.1016/J.JENVRAD.2011.03.018>
 44. Abbasi A, Mirekhtari F (2021) Estimation of natural gas contribution in indoor ^{222}Rn concentration level in residential houses. *J Radioanal Nucl Chem* 330:805–810. <https://doi.org/10.1007/S10967-021-08024-Z>
 45. ICRP. <https://www.icrp.org/publication.asp?id=ICRP%20Publication%20126>. Accessed 27 Jul 2023
 46. Boice J Jr, DA Cool U, Harrison UJ et al (2014). *Aims and Scope Subscriptions*. https://doi.org/10.1177/ANIB_43_3

Publisher's Note Springer Nature remains neutral with regard to jurisdictional claims in published maps and institutional affiliations.

Springer Nature or its licensor (e.g. a society or other partner) holds exclusive rights to this article under a publishing agreement with the

author(s) or other rightsholder(s); author self-archiving of the accepted manuscript version of this article is solely governed by the terms of such publishing agreement and applicable law.